Summer School on Complex Analysis and Passivity with Applications:

Applications of sum rules and physical bounds for passive systems

Daniel Sjöberg and Mats Gustafsson

Department of Electrical and Information Technology

Lund University, Sweden

Stockholm, August 2015

Outline

1. **Sum rules and physical bounds**
2. **Tools for obtaining physical bounds**
   - Composition of Herglotz (positive real) functions
   - Variational principles
3. **Applications**
   - Scattering
   - Antennas
   - Absorbers
   - Transmission blockage
   - High-impedance surfaces
   - Metamaterials
4. **Exercises**
5. **References**

Outline

Sum rules and physical bounds on passive systems

1. Identify a linear and passive system.
2. Construct a Herglotz (or similarly a positive real) function $h(z)$ that models the parameter of interest.
3. Investigate the asymptotic expansions of $h(z)$ as $z \hat{\to} 0$ and $z \hat{\to} \infty$.
4. Use integral identities for Herglotz functions to relate the dynamic properties to the asymptotic expansions.
5. Bound the integral.

Examples: Matching networks [2, 3], Radar absorbers [13], Antennas [8, 9, 5], Scattering [16, 1], High-impedance surfaces [7], Metamaterials [6],Extraordinary transmission [4],Periodic structures [11]

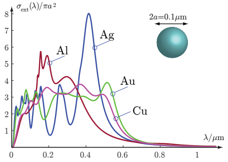

Cross sections of nano spheres.

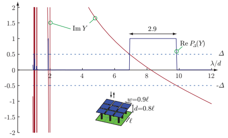

High-impedance surface.

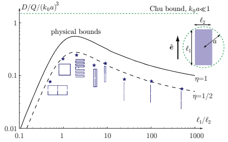

Antenna D/Q.

Integral identities for Herglotz functions

Herglotz functions with the symmetry $h(z) = -h^*(-z^*)$ (real-valued in the time domain) have asymptotic expansions ($N_0 \geq 0$ and $N_\infty \geq 0$)

$$\begin{cases} h(z) = \displaystyle\sum_{n=0}^{N_0} a_{2n-1} z^{2n-1} + \mathrm{o}(z^{2N_0-1}) & \text{as} \quad z \hat{\to} 0 \\ h(z) = \displaystyle\sum_{n=0}^{N_\infty} b_{1-2n} z^{1-2n} + \mathrm{o}(z^{1-2N_\infty}) & \text{as} \quad z \hat{\to} \infty \end{cases}$$

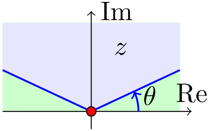

where $\hat{\to}$ denotes limits in the Stoltz domain $0 < \theta \leq \arg(z) \leq \pi - \theta$. They satisfy the identities ($1 - N_\infty \leq n \leq N_0$)

$$\lim_{\varepsilon \to 0^+} \lim_{y \to 0^+} \frac{2}{\pi} \int_{\varepsilon}^{\frac{1}{\varepsilon}} \frac{\operatorname{Im} h(x + \mathrm{i}y)}{x^{2n}} \, \mathrm{d}x = a_{2n-1} - b_{2n-1} = \begin{cases} -b_{2n-1} & n < 0 \\ a_{-1} - b_{-1} & n = 0 \\ a_1 - b_1 & n = 1 \\ a_{2n-1} & n > 1 \end{cases}$$

Bernland, Luger, Gustafsson, *Sum rules and constraints on passive systems*, J. Phys. A: Math. Theor., 2011.

Special cases

In the applications to follow, we will only use the following sum rules. For Herglotz functions with the asymptotics

$$\begin{cases} h(z) = a_{-1}z^{-1} + a_1 z + \mathrm{o}(z) \quad \text{as} \quad z \hat{\to} 0 \\ h(z) = b_1 z + b_{-1}z^{-1} + \mathrm{o}(z^{-1}) \quad \text{as} \quad z \hat{\to} \infty \end{cases}$$

the following sum rules apply:

$$\frac{2}{\pi}\int_0^\infty \operatorname{Im} h(x)\,\mathrm{d}x = a_{-1} - b_{-1}$$
$$\frac{2}{\pi}\int_0^\infty \frac{\operatorname{Im} h(x)}{x^2}\,\mathrm{d}x = a_1 - b_1$$

where the integrals are understood as the limits on the previous slide. Often, the variable x is identified as (angular) frequency ω.

Change of variables

With $x = \omega = 2\pi\mathrm{c}/\lambda$, the second integral can be transformed into

$$\frac{2}{\pi}\int_0^\infty \frac{\operatorname{Im} h(\omega)}{\omega^2}\,\mathrm{d}\omega = \frac{2}{\pi}\int_{\lambda=\infty}^{0} \left[\operatorname{Im} h\left(\frac{2\pi\mathrm{c}}{\lambda}\right)\right]\left(\frac{\lambda}{2\pi\mathrm{c}}\right)^2 \mathrm{d}\left(\frac{2\pi\mathrm{c}}{\lambda}\right)$$
$$= \frac{1}{\pi^2\mathrm{c}}\int_{\lambda=0}^{\infty} \operatorname{Im} h_\lambda(\lambda)\,\mathrm{d}\lambda$$

where $h_\lambda(\lambda) = h(2\pi\mathrm{c}/\lambda) = h(\omega)$. We often abuse notation and write only $h(\lambda)$. This implies the sum rules

$$\frac{2}{\pi}\int_0^\infty \operatorname{Im} h(\omega)\,\mathrm{d}\omega = a_{-1} - b_{-1}$$
$$\frac{1}{\pi^2\mathrm{c}}\int_0^\infty \operatorname{Im} h(\lambda)\,\mathrm{d}\lambda = a_1 - b_1$$

These are purely mathematical identities, which can be given physical interpretation.

Physical bounds

Given that $\operatorname{Im} h \geq 0$, we can estimate the integrals as

$$\int_0^\infty \operatorname{Im} h(\lambda)\,\mathrm{d}\lambda \geq \int_{\lambda_1}^{\lambda_2} \operatorname{Im} h(\lambda)\,\mathrm{d}\lambda \geq (\lambda_2 - \lambda_1) \min_{\lambda\in[\lambda_1,\lambda_2]} \operatorname{Im} h(\lambda)$$

This implies

$$(\lambda_2 - \lambda_1) \min_{\lambda\in[\lambda_1,\lambda_2]} \operatorname{Im} h(\lambda) \leq \pi^2 \mathrm{c}(a_1 - b_1)$$

With the interpretations

- $\lambda_2 - \lambda_1 =$ bandwidth
- $\min_{\lambda\in[\lambda_1,\lambda_2]} \operatorname{Im} h(\lambda) =$ performance level

we see that a physical interpretation of the sum rule is that

the product of bandwidth and performance level is bounded from above by low- and high-frequency asymptotics

Further interpretation is possible when h and the application are specified.

Different time conventions

In applications there is often a legacy of previous work to relate to. Therefore, we need to be able to handle analytic mappings in at least three complex half planes, and transform the results between them.

- Upper half plane to itself (passive systems with time convention $\mathrm{e}^{-\mathrm{i}\omega t}$, Herglotz functions $h(\omega)$).
- Right half plane to itself (passive systems with time convention e^{st}, positive real functions $p(s)$).
- Lower half plane to itself (passive systems with time convention $\mathrm{e}^{\mathrm{j}\omega t}$, (do they have a name?) functions $g(\omega)$).

$$h(\omega) = \mathrm{j}p(\mathrm{j}\omega^*)^* \quad \Leftrightarrow \quad p(s) = \mathrm{j}h(\mathrm{j}s^*)^*$$

$$g(\omega) = -\mathrm{j}p(\mathrm{j}\omega) \quad \Leftrightarrow \quad p(s) = \mathrm{j}g(-\mathrm{j}s)$$

$$g(\omega) = h(\omega^*)^* \quad \Leftrightarrow \quad h(\omega) = g(\omega^*)^*$$

Outline

Outline

Composition of Herglotz (positive real) functions

A useful property of Herglotz/PR functions is that they can be composed to find new Herglotz/PR functions. For instance, with $p_1(s)$ and $p_2(s)$ being positive real functions, the following combinations are also positive real:

$$
\begin{array}{ccc}
p_2(p_1(s)) & \sqrt{p_1(s)p_2(s)} & \sqrt{p_1(s)/p_2(s))} \\
1/p_1(s) & p_1(1/s) & p_1(s)+p_2(s)
\end{array}
$$

A typical case can be an investigation of negative refractive index, $n(s) \approx -1$. The positive real function

$$p(s) = s(n(s)+1)$$

is then close to zero when $n(s) \approx -1$. The function

$$\frac{2}{\pi}\arctan\left(\frac{\varDelta}{p(s)}\right)$$

can be shown to have a real part close to unity when $|p(s)| < \varDelta$.

Outline

Computation of polarizability

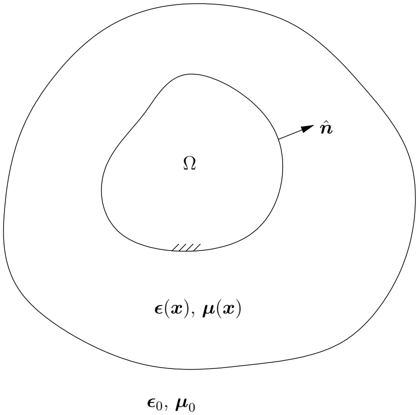

$$\boldsymbol{p} = \epsilon_0 \boldsymbol{\gamma}_{\mathrm{e}} \cdot \boldsymbol{E}_0 = \int_{\mathbb{R}^3 \setminus \Omega} (\boldsymbol{\epsilon} - \boldsymbol{\epsilon}_0) \cdot \boldsymbol{E} \,\mathrm{d}V + \oint_{\partial\Omega} \boldsymbol{r} \hat{\boldsymbol{n}} \cdot \boldsymbol{D} \,\mathrm{d}S$$

$$\boldsymbol{m} = \mu_0^{-1} \boldsymbol{\gamma}_{\mathrm{m}} \cdot \boldsymbol{B}_0 = \int_{\mathbb{R}^3 \setminus \Omega} (\boldsymbol{\mu}_0^{-1} - \boldsymbol{\mu}^{-1}) \cdot \boldsymbol{B} \,\mathrm{d}V + \frac{1}{2} \oint_{\partial\Omega} \boldsymbol{r} \times (\hat{\boldsymbol{n}} \times \boldsymbol{H}) \,\mathrm{d}S$$

Two ways of solving the electrostatic equations

The electrostatic problem can be solved using two different potentials:

$$\nabla \times \boldsymbol{E} = \boldsymbol{0} \qquad \Rightarrow \qquad \boldsymbol{E} = \boldsymbol{E}_0 - \nabla\varphi$$
$$\nabla \cdot \boldsymbol{D} = 0 \qquad \Rightarrow \qquad \boldsymbol{D} = \boldsymbol{D}_0 + \nabla \times \boldsymbol{F}$$

This provides two different expressions for the energy:

$$J(\varphi, \boldsymbol{E}_0) = \int \left[(\boldsymbol{E}_0 - \nabla\varphi) \cdot \boldsymbol{\epsilon}(\boldsymbol{r}) \cdot (\boldsymbol{E}_0 - \nabla\varphi) - \epsilon_0 |\boldsymbol{E}_0|^2\right] \, \mathrm{d}V$$

$$K(\boldsymbol{F}, \boldsymbol{D}_0) = \int \left[(\boldsymbol{D}_0 + \nabla \times \boldsymbol{F}) \cdot \boldsymbol{\epsilon}(\boldsymbol{r})^{-1} \cdot (\boldsymbol{D}_0 + \nabla \times \boldsymbol{F}) - \epsilon_0^{-1} |\boldsymbol{D}_0|^2\right] \, \mathrm{d}V$$

It can be shown [14] that for all test functions φ and $\boldsymbol{F}$ (they do not need to solve the electrostatic equations), we have

$$\epsilon_0 \boldsymbol{E}_0 \cdot \boldsymbol{\gamma}_\mathrm{e} \cdot \boldsymbol{E}_0 \leq J(\varphi, \boldsymbol{E}_0), \quad -\epsilon_0^{-1} \boldsymbol{D}_0 \cdot \boldsymbol{\gamma}_\mathrm{e} \cdot \boldsymbol{D}_0 \leq K(\boldsymbol{F}, \boldsymbol{D}_0)$$

There exist unique minimizing potentials φ_0 and $\boldsymbol{F}_0$, which are the solutions to the electrostatic equations.

Two ways of solving the electrostatic equations

The electrostatic problem can be solved using two different potentials:

$$\begin{aligned} \nabla \times \boldsymbol{E} = \boldsymbol{0} \qquad &\Rightarrow \qquad \boldsymbol{E} = \boldsymbol{E}_0 - \nabla\varphi \\ \nabla \cdot \boldsymbol{D} = 0 \qquad &\Rightarrow \qquad \boldsymbol{D} = \boldsymbol{D}_0 + \nabla \times \boldsymbol{F} \end{aligned}$$

This provides two different expressions for the energy:

$$J(\varphi, \boldsymbol{E}_0) = \int \left[(\boldsymbol{E}_0 - \nabla\varphi) \cdot \boldsymbol{\epsilon}(\boldsymbol{r}) \cdot (\boldsymbol{E}_0 - \nabla\varphi) - \epsilon_0 |\boldsymbol{E}_0|^2\right] \,\mathrm{d}V$$

$$K(\boldsymbol{F}, \boldsymbol{D}_0) = \int \left[(\boldsymbol{D}_0 + \nabla \times \boldsymbol{F}) \cdot \boldsymbol{\epsilon}(\boldsymbol{r})^{-1} \cdot (\boldsymbol{D}_0 + \nabla \times \boldsymbol{F}) - \epsilon_0^{-1} |\boldsymbol{D}_0|^2\right] \,\mathrm{d}V$$

It can be shown [14] that for all test functions φ and $\boldsymbol{F}$ (they do not need to solve the electrostatic equations), we have

$$\epsilon_0 \boldsymbol{E}_0 \cdot \boldsymbol{\gamma}_\mathrm{e} \cdot \boldsymbol{E}_0 \leq J(\varphi, \boldsymbol{E}_0), \quad -\epsilon_0^{-1} \boldsymbol{D}_0 \cdot \boldsymbol{\gamma}_\mathrm{e} \cdot \boldsymbol{D}_0 \leq K(\boldsymbol{F}, \boldsymbol{D}_0)$$

There exist unique minimizing potentials φ_0 and $\boldsymbol{F}_0$, which are the solutions to the electrostatic equations.

If we can **guess** solutions φ and $\boldsymbol{F}$, we can bound $\boldsymbol{\gamma}_\mathrm{e}$!

Example: the Wiener bounds

Introduce the relative permittivity matrix as $\boldsymbol{\epsilon}_{\mathrm{r}}(\boldsymbol{r}) = \boldsymbol{\epsilon}(\boldsymbol{r})/\epsilon_0$. The simplest guess is $\varphi = 0$ and $\boldsymbol{F} = \mathbf{0}$. We then have

$$J(0, \boldsymbol{E}_0) = \epsilon_0 \boldsymbol{E}_0 \cdot \int (\boldsymbol{\epsilon}_{\mathrm{r}}(\boldsymbol{r}) - \mathbf{I}) \, \mathrm{d}V \cdot \boldsymbol{E}_0$$

$$K(\mathbf{0}, \boldsymbol{D}_0) = -\epsilon_0^{-1} \boldsymbol{D}_0 \cdot \int (\mathbf{I} - \boldsymbol{\epsilon}_{\mathrm{r}}(\boldsymbol{r})^{-1}) \, \mathrm{d}V \cdot \boldsymbol{D}_0$$

Setting $\boldsymbol{D}_0 = \epsilon_0 \boldsymbol{E}_0$, this implies (known as the Wiener bounds in homogenization theory)

$$\int (\mathbf{I} - \boldsymbol{\epsilon}_{\mathrm{r}}(\boldsymbol{r})^{-1}) \, \mathrm{d}V \leq \boldsymbol{\gamma}_{\mathrm{e}} \leq \int (\boldsymbol{\epsilon}_{\mathrm{r}}(\boldsymbol{r}) - \mathbf{I}) \, \mathrm{d}V$$

where the inequalities are interpreted in terms of quadratic forms, that is, $\boldsymbol{\gamma}_{\mathrm{e}} \geq 0$ means $\boldsymbol{E}_0 \cdot \boldsymbol{\gamma}_{\mathrm{e}} \cdot \boldsymbol{E}_0 \geq 0$ for all $\boldsymbol{E}_0$.

Slightly more advanced: with PEC inclusions

Let Ω be a PEC region. The set of admissible potentials $\mathcal{A}_\varphi$ must then be restricted as follows:

$$J(\varphi, \boldsymbol{E}_0) = \int_{\mathbb{R}^3} \left[(\boldsymbol{E}_0 - \nabla\varphi) \cdot \boldsymbol{\epsilon}(\boldsymbol{r}) \cdot (\boldsymbol{E}_0 - \nabla\varphi) - \epsilon_0 |\boldsymbol{E}_0|^2 \right] \mathrm{d}V$$

$$\mathcal{A}_\varphi = \left\{ \varphi \in H_1(\mathbb{R}^3 \setminus \Omega) \;\middle|\; \begin{array}{rl} \boldsymbol{E}_0 - \nabla\varphi = \boldsymbol{0} & \boldsymbol{r} \in \Omega \\ \hat{\boldsymbol{n}} \times (\boldsymbol{E}_0 - \nabla\varphi) = \boldsymbol{0} & \boldsymbol{r} \in \partial\Omega \end{array} \right\}$$

and the polarizability is the minimum

$$\epsilon_0 \boldsymbol{E}_0 \cdot \boldsymbol{\gamma}_\mathrm{e} \cdot \boldsymbol{E}_0 = \min_{\varphi \in \mathcal{A}_\varphi} J(\varphi, \boldsymbol{E}_0)$$

Similar reasoning applies to the dual functional $K(\boldsymbol{F}, \boldsymbol{D}_0)$, but we mostly use the functional J since it corresponds to an upper bound.

Variational result for permittivity

Consider two objects with different material properties:

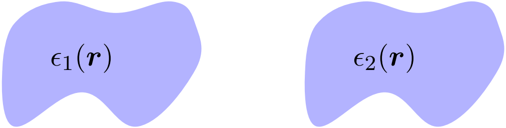

Assuming that $\boldsymbol{\epsilon}_2(\boldsymbol{r}) \geq \boldsymbol{\epsilon}_1(\boldsymbol{r})$ everywhere, we have

$$J_2(\varphi, \boldsymbol{E}_0) - J_1(\varphi, \boldsymbol{E}_0) = \int_{\mathbb{R}^3} (\boldsymbol{E}_0 - \nabla\varphi) \cdot (\boldsymbol{\epsilon}_2(\boldsymbol{r}) - \boldsymbol{\epsilon}_1(\boldsymbol{r})) \cdot (\boldsymbol{E}_0 - \nabla\varphi) \, \mathrm{d}V$$

which is nonnegative for all φ and $\boldsymbol{E}_0$. Choosing $\varphi = \varphi_2$, where φ_2 minimizes J_2, this means

$$\epsilon_0 \boldsymbol{E}_0 \cdot (\boldsymbol{\gamma}_{\mathrm{e2}} - \boldsymbol{\gamma}_{\mathrm{e1}}) \cdot \boldsymbol{E}_0 \geq J_2(\varphi_2, \boldsymbol{E}_0) - J_1(\varphi_2, \boldsymbol{E}_0) \geq 0$$

This is summarized as the variational result

If the permittivity is increased, the polarizability can not decrease.

High-contrast polarizability

We often want to estimate the polarizability of *any* structure contained in a certain region Ω.

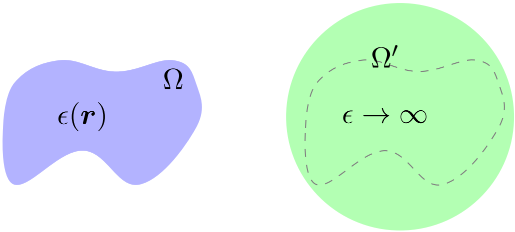

The region Ω' contains Ω, and they can coincide. The variational principle provides the upper bound

$$\boldsymbol{\gamma_{\mathrm{e}} \leq \gamma_{\infty}}$$

Example: the polarizability of a metal sphere with radius a is $\gamma_{\infty} = 4\pi a^3$. Any structure contained in a sphere with radius a then has $\gamma_{\mathrm{e}} \leq 4\pi a^3$.

Outline

1. **Sum rules and physical bounds**
2. **Tools for obtaining physical bounds**
   - Composition of Herglotz (positive real) functions
   - Variational principles
3. **Applications**
   - Scattering
   - Antennas
   - Absorbers
   - Transmission blockage
   - High-impedance surfaces
   - Metamaterials
4. **Exercises**
5. **References**

Outline

Sum rules in scattering theory

Scattering theory is a nice application for sum rules. We will discuss scattering in 3, 2, and 1 spatial dimensions, and show that in each of them the following sum rule applies:

$$\int_0^\infty \sigma^{\mathrm{ext}}(\lambda)\,\mathrm{d}\lambda = \pi^2\gamma$$

where the extinction cross section σ^{ext} is the sum of the absorption and scattering cross sections, and γ is the sum of the electric and magnetic static polarizabilities of the scatterer.

This means the total electromagnetic interaction, summed over all wavelengths, is determined by a property that can be computed from a static problem.

Scattering in 3D

A plane wave $\boldsymbol{E}^{\mathrm{i}}(\boldsymbol{r}) = \boldsymbol{E}_0 \mathrm{e}^{-\mathrm{j}\boldsymbol{k}\cdot\boldsymbol{r}}$, $\boldsymbol{H}^{\mathrm{i}}(\boldsymbol{r}) = \frac{1}{\eta_0}\hat{\boldsymbol{k}} \times \boldsymbol{E}^{\mathrm{i}}(\boldsymbol{r})$, impinges on a scattering object enclosed by a surface S.

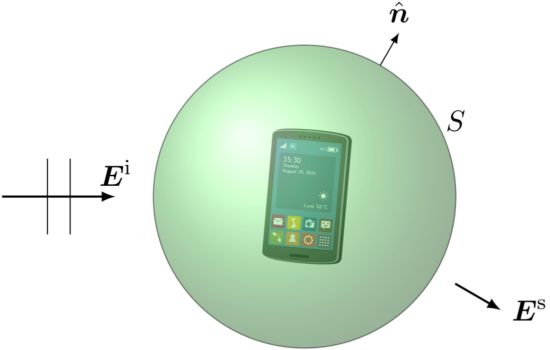

Scattered power: $$P^{\mathrm{s}} = \frac{1}{2}\mathrm{Re}\oint_S \hat{\boldsymbol{n}} \cdot (\boldsymbol{E}^{\mathrm{s}} \times \boldsymbol{H}^{\mathrm{s}*})\,\mathrm{d}S$$

Absorbed power: $$P^{\mathrm{a}} = -\frac{1}{2}\mathrm{Re}\oint_S \hat{\boldsymbol{n}} \cdot (\boldsymbol{E} \times \boldsymbol{H}^{*})\,\mathrm{d}S$$

Extinct power

The extinct power is the sum of scattered and absorbed power:

$$P^{\mathrm{ext}} = P^{\mathrm{s}} + P^{\mathrm{a}} = \frac{1}{2}\,\mathrm{Re}\int_S \hat{\boldsymbol{n}}\cdot\left(\boldsymbol{E}^{\mathrm{s}}\times\boldsymbol{H}^{\mathrm{s}*} - \boldsymbol{E}\times\boldsymbol{H}^{*}\right)\mathrm{d}S$$

$$= \frac{1}{2}\,\mathrm{Re}\int_S \hat{\boldsymbol{n}}\cdot\left(\boldsymbol{E}^{\mathrm{s}}\times\boldsymbol{H}^{\mathrm{s}*} - (\boldsymbol{E}^{\mathrm{i}}+\boldsymbol{E}^{\mathrm{s}})\times(\boldsymbol{H}^{\mathrm{i}}+\boldsymbol{H}^{\mathrm{s}})^{*}\right)\mathrm{d}S$$

$$= -\frac{1}{2}\,\mathrm{Re}\int_S \hat{\boldsymbol{n}}\cdot\left(\boldsymbol{E}^{\mathrm{i}}\times\boldsymbol{H}^{\mathrm{s}*} - \boldsymbol{E}^{\mathrm{s}}\times\boldsymbol{H}^{\mathrm{i}*}\right)\mathrm{d}S$$

Here, we used $\frac{1}{2}\,\mathrm{Re}\int_S \hat{\boldsymbol{n}}\cdot(\boldsymbol{E}^{\mathrm{i}}\times\boldsymbol{H}^{\mathrm{i}*})\,\mathrm{d}S = 0$. When the incident field is a plane wave, this becomes ($\boldsymbol{E}^{\mathrm{s}} \sim \boldsymbol{F}\mathrm{e}^{-\mathrm{j}kr}/r$, $r\to\infty$)

$$P^{\mathrm{ext}} = \frac{1}{2}\,\mathrm{Re}\left\{\boldsymbol{E}_0^{*}\cdot\int_S\left[\hat{\boldsymbol{n}}\times\boldsymbol{H}^{\mathrm{s}} + \frac{1}{\eta_0}\hat{\boldsymbol{k}}\times(\hat{\boldsymbol{n}}\times\boldsymbol{E}^{\mathrm{s}})\right]\mathrm{e}^{\mathrm{j}\boldsymbol{k}\cdot\boldsymbol{r}}\,\mathrm{d}S\right\}$$

$$= \frac{1}{2}\,\mathrm{Re}\left\{-\frac{4\pi}{\mathrm{j}k\eta_0}\boldsymbol{E}_0^{*}\cdot\frac{\mathrm{j}k}{4\pi}\hat{\boldsymbol{k}}\times\int_S\left[\hat{\boldsymbol{k}}\times(\hat{\boldsymbol{n}}\times\eta_0\boldsymbol{H}^{\mathrm{s}}) + \boldsymbol{E}^{\mathrm{s}}\times\hat{\boldsymbol{n}}\right]\mathrm{e}^{\mathrm{j}\boldsymbol{k}\cdot\boldsymbol{r}}\,\mathrm{d}S\right\}$$

$$= \frac{1}{2}\,\mathrm{Re}\left\{-\frac{4\pi}{\mathrm{j}k\eta_0}\boldsymbol{E}_0^{*}\cdot\boldsymbol{F}(\hat{\boldsymbol{k}})\right\}$$

Optical theorem in 3D

With the incident power flux $S^{\mathrm{i}} = \frac{|\boldsymbol{E}_0|^2}{2\eta_0}$ we obtain the extinction cross section

$$\boxed{\sigma^{\mathrm{ext}} = \frac{P^{\mathrm{ext}}}{S^{\mathrm{i}}} = \operatorname{Re}\left\{-\frac{4\pi}{\mathrm{j}k}\frac{\boldsymbol{E}_0^* \cdot \boldsymbol{F}(\hat{\boldsymbol{k}})}{|\boldsymbol{E}_0|^2}\right\}}$$

This is remarkable since the (extinct) power, a quadratic quantity, depends linearly on the scattered field through $\boldsymbol{F}(\hat{\boldsymbol{k}})$. The forward scattering far field is analytic in a half plane due to causality.

Our prototype Herglotz function is then (switching to time convention $\mathrm{e}^{-\mathrm{i}\omega t}$)

$$\boxed{h_{\mathrm{3D}}(k) = \frac{4\pi}{k}\frac{\boldsymbol{E}_0^* \cdot \boldsymbol{F}(k;\hat{\boldsymbol{k}})}{|\boldsymbol{E}_0|^2}}$$

where $\operatorname{Im} h = \sigma^{\mathrm{ext}} \geq 0$.

Scattering in 2D

The baseline geometry is translational invariant along z:

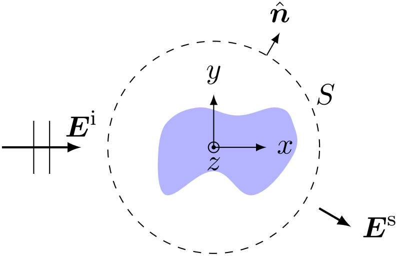

But it can also be a geometry periodic in z, for instance realized between two parallel plates:

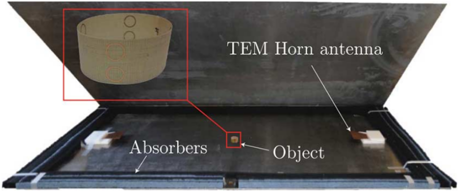

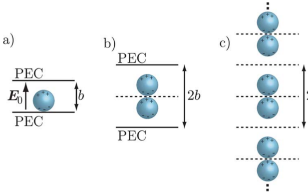

Optical theorem in 2D

In a two-dimensional geometry we only need to change the definition of the far field amplitude ($\boldsymbol{E}^{\mathrm{s}} \sim \boldsymbol{f}\sqrt{\frac{2}{\pi \mathrm{j} k\rho}}\mathrm{e}^{-\mathrm{j}k\rho}$, $\rho \to \infty$)

$$P^{\mathrm{ext}} = \frac{1}{2}\,\mathrm{Re}\left\{\boldsymbol{E}_0^* \cdot \int_S \left[\hat{\boldsymbol{n}} \times \boldsymbol{H}^{\mathrm{s}} + \frac{1}{\eta_0}\hat{\boldsymbol{k}} \times (\hat{\boldsymbol{n}} \times \boldsymbol{E}^{\mathrm{s}})\right] \mathrm{e}^{\mathrm{j}\boldsymbol{k}\cdot\boldsymbol{r}}\,\mathrm{d}S\right\}$$

$$= \frac{1}{2}\,\mathrm{Re}\left\{-\frac{4b}{\eta_0 \mathrm{j}k}\boldsymbol{E}_0^* \cdot \frac{\mathrm{j}k}{4b}\hat{\boldsymbol{k}} \times \int_0^b \oint_C \left[\hat{\boldsymbol{k}} \times (\hat{\boldsymbol{n}} \times \eta_0 \boldsymbol{H}^{\mathrm{s}}) + \boldsymbol{E}^{\mathrm{s}} \times \hat{\boldsymbol{n}}\right] \mathrm{e}^{\mathrm{j}\boldsymbol{k}\cdot\boldsymbol{r}}\,\mathrm{d}\ell\,\mathrm{d}z\right\}$$

$$= \frac{1}{2}\,\mathrm{Re}\left\{-\frac{4b}{\eta_0 \mathrm{j}k}\boldsymbol{E}_0^* \cdot \boldsymbol{f}(\hat{\boldsymbol{k}})\right\}$$

The extinction cross section is then (with incident power flux $S^{\mathrm{i}} = \frac{|\boldsymbol{E}_0|^2}{2\eta_0}$)

$$\sigma_{\mathrm{2D}}^{\mathrm{ext}} = \frac{P^{\mathrm{ext}}}{S^{\mathrm{i}}} = \mathrm{Re}\left\{-\frac{4b}{\mathrm{j}k}\frac{\boldsymbol{E}_0^* \cdot \boldsymbol{f}(\hat{\boldsymbol{k}})}{|\boldsymbol{E}_0|^2}\right\}$$

$$h_{\mathrm{2D}}(k) = \frac{4b}{k}\frac{\boldsymbol{E}_0^* \cdot \boldsymbol{f}(\hat{\boldsymbol{k}})}{|\boldsymbol{E}_0|^2}$$

Scattering in 1D

The baseline geometry is translational invariant along x and y:

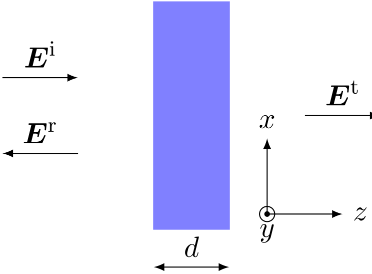

But it can also be a geometry periodic in x and y:

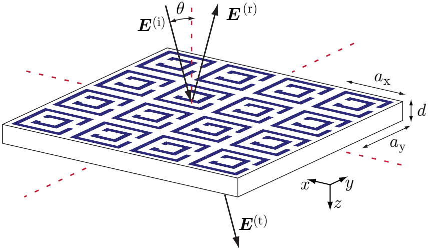

Optical theorem in 1D

The different powers are (where T is the transmission coefficient for the fundamental mode, P_1^{t} is the transmitted power in remaining modes, and P^{r} is the total reflected power)

Incident power:	$P^{\mathrm{i}} = AS^{\mathrm{i}} = A\lvert\boldsymbol{E}_0\rvert^2/(2\eta_0)$
Scattered power:	$P^{\mathrm{s}} = P^{\mathrm{r}} + \lvert 1-T\rvert^2 P^{\mathrm{i}} + P_1^{\mathrm{t}}$
Absorbed power:	$P^{\mathrm{a}} = P^{\mathrm{i}} - P^{\mathrm{r}} - \lvert T\rvert^2 P^{\mathrm{i}} - P^{\mathrm{t}}$

The extinct power is

$$\begin{aligned} P^{\mathrm{ext}} &= P^{\mathrm{s}} + P^{\mathrm{a}} = P^{\mathrm{r}} + \lvert 1-T\rvert^2 P^{\mathrm{i}} + P_1^{\mathrm{t}} + P^{\mathrm{i}} - P^{\mathrm{r}} - \lvert T\rvert^2 P^{\mathrm{i}} - P_1^{\mathrm{t}} \\ &= (1 - 2\,\mathrm{Re}\,T + \lvert T\rvert^2)P^{\mathrm{i}} + P^{\mathrm{i}} - \lvert T\rvert^2 P^{\mathrm{i}} = 2\,\mathrm{Re}\{1-T\}P^{\mathrm{i}} \end{aligned}$$

The extinction cross section per unit cell with area A is then

$$\boxed{\sigma_{\mathrm{1D}}^{\mathrm{ext}} = \frac{P^{\mathrm{ext}}}{S^{\mathrm{i}}} = 2\,\mathrm{Re}\{1-T\}A} \qquad \boxed{h_{\mathrm{1D}}(k) = 2\mathrm{i}(1-T(k))A}$$

Low frequency asymptotics

In the low frequency limit, the forward scattering amplitudes are

$$h_{n\mathrm{D}}(k) = k\gamma + \mathrm{o}(k), \quad n = 1, 2, 3$$

where γ is the sum of the (static) electric and magnetic polarizabilities

$$\gamma = \frac{\boldsymbol{E}_0^* \cdot \boldsymbol{\gamma}_{\mathrm{e}} \cdot \boldsymbol{E}_0}{|\boldsymbol{E}_0|^2} + \frac{\boldsymbol{H}_0^* \cdot \boldsymbol{\gamma}_{\mathrm{m}} \cdot \boldsymbol{H}_0}{|\boldsymbol{H}_0|^2}$$

defined by solving the static Maxwell's equations and relating the incident field to the induced dipole moments:

$$\boldsymbol{p} = \epsilon_0 \boldsymbol{\gamma}_{\mathrm{e}} \cdot \boldsymbol{E}_0, \quad \boldsymbol{m} = \boldsymbol{\gamma}_{\mathrm{m}} \cdot \boldsymbol{H}_0$$

Note: this excludes cases where a net current flows through the structures in the low frequency limit, that is, we only consider disconnected conducting regions.

High frequency asympotics

In the high frequency limit the forward scattering is expected to be proportional to the projected area of the scatterer, implying

$$h_{n\mathrm{D}}(k) = \mathrm{O}(1), \quad k \to \infty$$

where $n = 1, 2, 3$.

Sum rules for extinction cross section

With the asymptotics

$$
\begin{aligned}
h_{n\mathrm{D}}(k) &= k\gamma + \mathrm{o}(k) && k \to 0 \\
h_{n\mathrm{D}}(k) &= \mathrm{O}(1) && k \to \infty
\end{aligned}
$$

we have the sum rule (where $\sigma^{\mathrm{ext}} = \mathrm{Im}(h_{n\mathrm{D}})$)

$$\int_0^\infty \sigma^{\mathrm{ext}}(\lambda; \hat{\boldsymbol{k}}, \boldsymbol{E}_0)\,\mathrm{d}\lambda = \pi^2\gamma$$

for all dimensions $n = 1, 2, 3$. This implies the physical bound

$$\boxed{(\lambda_2 - \lambda_1)\sigma^{\mathrm{ext}}_{\mathrm{min}} \leq \pi^2\gamma \leq \pi^2\gamma_\infty}$$

where γ_∞ is the high-contrast polarizability for any shape containing the scatterer.

Experimental results 3D [17]

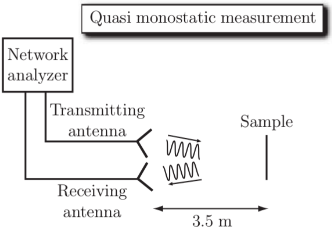

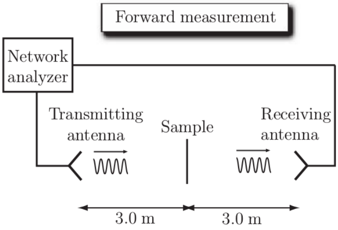

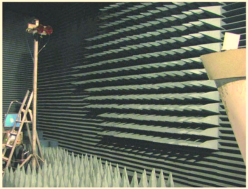

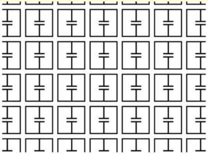

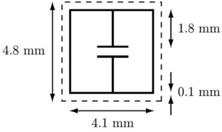

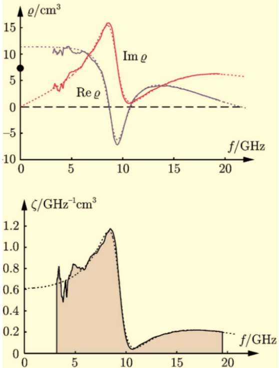

Experimental results parallel plate [18]

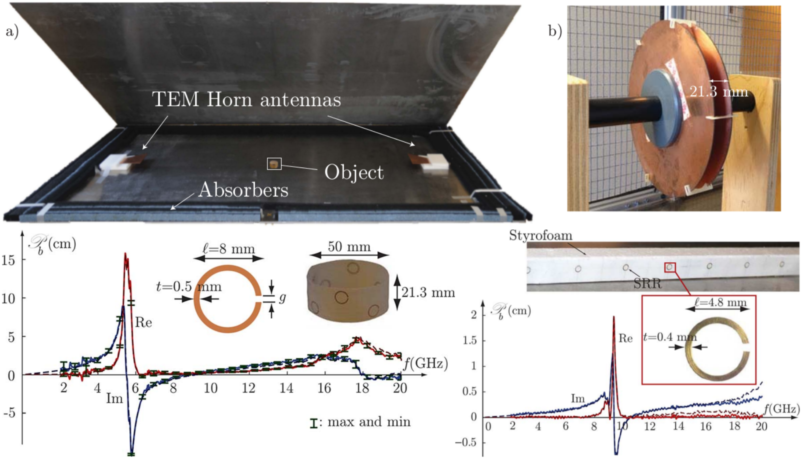

Estimates of γ_e	Left (2D)	Right (1D)
$\frac{1}{\pi^2}\int_{\lambda_1}^{\lambda_2} \sigma^{\text{ext}}(\lambda)\,\mathrm{d}\lambda$ / cm^3	2.75	0.111 (0.208)
γ_e from capacitor / cm^3	3.65	0.196

Outline

Identification of antenna parameters

The scattering sum rule

$$\int_0^\infty \sigma^{\mathrm{ext}}(\lambda)\,\mathrm{d}\lambda = \pi^2\gamma$$

can be put in terms of antenna parameters after observing [8]

$$\sigma^{\mathrm{ext}} \geq \sigma^{\mathrm{a}} = (1-|\varGamma|^2)\sigma_0^{\mathrm{a}} = \frac{1}{4\pi}(1-|\varGamma|^2)\lambda^2 D(\lambda)$$

Here, we used reciprocity to relate the absorption cross section to the directivity, including mismatch losses. Since the gain $G \leq D$, we have

$$\frac{1}{4\pi}\int_0^\infty (1-|\varGamma|^2)G(\lambda)\lambda^2\,\mathrm{d}\lambda \leq \int_0^\infty \sigma^{\mathrm{ext}}(\lambda)\,\mathrm{d}\lambda = \pi^2\gamma$$

Estimating the integral

Introduce the minimum partial realized gain in the interval $\Lambda = [\lambda_1, \lambda_2]$ as

$$G_\Lambda = \min_{\lambda\in\Lambda}(1 - |\mathit{\Gamma}(\lambda)|^2)G(\lambda)$$

to find the estimate [8]

$$\int_0^\infty (1 - |\mathit{\Gamma}|^2)G\lambda^2 \,\mathrm{d}\lambda \geq G_\Lambda \int_{\lambda_1}^{\lambda_2} \lambda^2 \,\mathrm{d}\lambda \geq G_\Lambda B \lambda_0^3$$

where $\lambda_0 = (\lambda_1 + \lambda_2)/2$ and $B = (\lambda_2 - \lambda_1)/\lambda_0$. This implies the physical bound

$$\boxed{BG_\Lambda \leq \frac{4\pi^3}{\lambda_0^3}\gamma = \frac{1}{2}k_0^3\gamma \leq \frac{1}{2}k_0^3\gamma_\infty}$$

where γ_∞ is the high-contrast polarizability of any shape enclosing the antenna.

Illustrations of the bound [9]

In terms of the directivity D and quality factor Q, we have

$$\boxed{\frac{D}{Q} \leq \frac{\eta}{2\pi} k_0^3 \gamma} \qquad \left(\text{where} \quad \eta = \frac{\int_0^\infty \sigma^{\mathrm{a}}(\lambda)\,\mathrm{d}\lambda}{\int_0^\infty \sigma^{\mathrm{ext}}(\lambda)\,\mathrm{d}\lambda} \right)$$

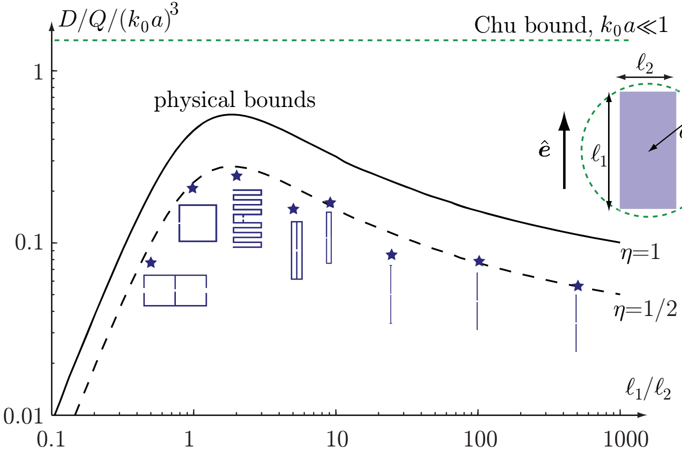

Outline

Rozanov's bound for absorbers

The typical case of an absorber is a metal backed structure with thickness d.

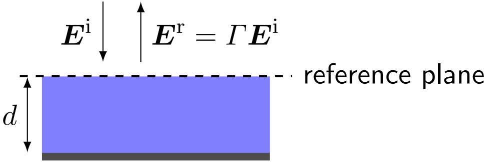

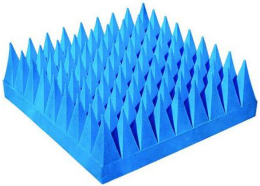

Rozanov [13] showed that

$$\boxed{(\lambda_2 - \lambda_1)\mathit{\Gamma}_0 \le 172 d \mu_{\mathrm{s}}}$$

where $\mathit{\Gamma}_0$ is the minimum allowed return loss in dB for $\lambda \in [\lambda_1, \lambda_2]$, and μ_{s} is the static relative permeability. For wide band absorbers we have $\lambda_{\max} = \lambda_2 \gg \lambda_1$, and

$$\boxed{\lambda_{\max}\mathit{\Gamma}_0 \le 172 d \mu_{\mathrm{s}}}$$

Rozanov's bound

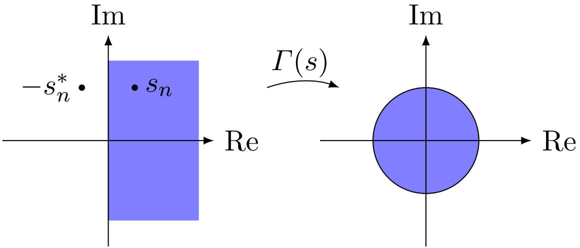

The reflection coefficient maps the right half plane to the unit circle. In case $\mathit{\Gamma}(s_n) = 0$ for some $\{s_n\}_{n=1}^N$ in the right half plane, we introduce the function (which satisfies $|\mathit{\Gamma}'(\mathrm{j}\omega)| = |\mathit{\Gamma}(\mathrm{j}\omega)|$)

$$\mathit{\Gamma}'(s) = \mathit{\Gamma}(s)\frac{(s+s_1^*)\cdots(s+s_N^*)}{(s-s_1)\cdots(s-s_N)}$$

where the (possible) zeros of $\mathit{\Gamma}(s)$ have been reflected in the imaginary axis. $\mathit{\Gamma}'(s)$ has neither zeros nor poles for s in the right half plane. Then, $\log(1/\mathit{\Gamma}'(s))$ is a positive real function.

Behavior of the Blaschke product

The logarithm is

$$\log \frac{1}{\Gamma'(s)} = \log \frac{1}{\Gamma(s)} + \log \left(\frac{(s-s_1)\cdots(s-s_N)}{(s+s_1^*)\cdots(s+s_N^*)} \right)$$

and since

$$\log \left(\frac{s-s_n}{s+s_n^*} \right) = \begin{cases} -2s \,\mathrm{Re}\, \frac{1}{s_n} + \mathrm{O}(s^2) & s \to 0 \\ -2\frac{1}{s} \,\mathrm{Re}\, s_n + \mathrm{O}(1/s^2) & s \to \infty \end{cases}$$

we have

$$\log \frac{1}{\Gamma'(s)} = \begin{cases} \log \frac{1}{\Gamma(s)} - 2s \,\mathrm{Re} \sum_{n=1}^{N} \frac{1}{s_n} & s \to 0 \\ \log \frac{1}{\Gamma(s)} - 2\frac{1}{s} \,\mathrm{Re} \sum_{n=1}^{N} s_n & s \to \infty \end{cases}$$

On the frequency axis $s = \mathrm{j}\omega$ we have $\left| \frac{s+s_1^*}{s-s_1} \right| = \left| \frac{\mathrm{j}\omega+s_1^*}{\mathrm{j}\omega-s_1} \right| = 1$, which implies

$$\mathrm{Re} \left\{ \log \frac{1}{\Gamma'(\mathrm{j}\omega)} \right\} = \ln \left| \frac{1}{\Gamma'(\mathrm{j}\omega)} \right| = \ln \left| \frac{1}{\Gamma(\mathrm{j}\omega)} \right|$$

Visualization of the transformations

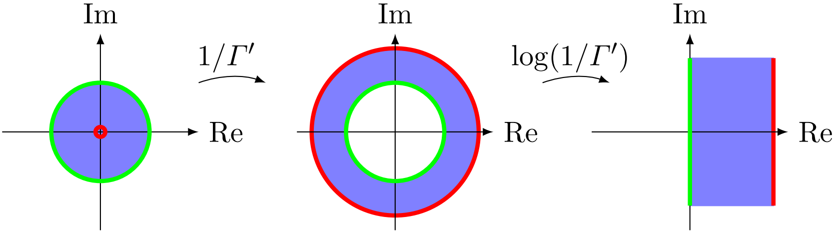

The origin $\Gamma \approx 0$ has now been transformed to a region with a large real part.

Low- and high-frequency asympotics

The low- and high-frequency asymptotics are

$$\mathit{\Gamma}(s) = \begin{cases} -1 + \frac{2ds}{\mathrm{c}}(1 + \frac{\gamma_{\mathrm{m}}}{Ad}) + \mathrm{O}(s^2) & s \to 0 \\ -\mathrm{e}^{-(n_\infty - 1)2ds/\mathrm{c}} + \mathrm{O}(1/s) & s \to \infty \end{cases}$$

where γ_{m}/A is the magnetic polarizability per unit area of the absorber. This implies

$$\log(1/\mathit{\Gamma}'(s)) = \begin{cases} \frac{2ds}{\mathrm{c}}(1 + \frac{\gamma_{\mathrm{m}}}{Ad}) - 2s\,\mathrm{Re}\sum_{n=1}^{N} \frac{1}{s_n} + \mathrm{O}(s^2) & s \to 0 \\ (n_\infty - 1)2ds/\mathrm{c} - 2\frac{1}{s}\,\mathrm{Re}\sum_{n=1}^{N} s_n + \mathrm{O}(1) & s \to \infty \end{cases}$$

and we immediately have the sum rule

$$\int_0^\infty \mathrm{Re}\left\{\log\frac{1}{\mathit{\Gamma}'(\lambda)}\right\} \mathrm{d}\lambda = \pi^2 2d\left(1 + \frac{\gamma_{\mathrm{m}}}{Ad} - 2\,\mathrm{Re}\sum_{n=1}^{N}\frac{\mathrm{c}/d}{s_n} - (n_\infty - 1)\right)$$

Simplifications

Since $\mathrm{Re}\left\{\log\frac{1}{\Gamma'(\lambda)}\right\} = \ln\frac{1}{|\Gamma(\lambda)|}$, $\mathrm{Re}\,\frac{1}{s_n} > 0$ for s_n in the right half plane, and $n_\infty \geq 1$ due to special relativity, we have

$$\boxed{\int_0^\infty \ln\frac{1}{|\Gamma(\lambda)|}\,\mathrm{d}\lambda \leq \pi^2 2d\left(1+\frac{\gamma_\mathrm{m}}{Ad}\right)}$$

Define the static permeability by $\mu_\mathrm{s} = 1 + \gamma_\mathrm{m}/(Ad)$, and the dB-scale return loss by $\ln\frac{1}{|\Gamma|} = \ln(10)|\Gamma_\mathrm{dB}|/20$. We can then estimate the integral by

$$\boxed{(\lambda_2 - \lambda_1)\Gamma_0 \leq \frac{20}{\ln 10}\pi^2 2d\mu_\mathrm{s} = 172 d\mu_\mathrm{s}}$$

where $\Gamma_0 = \min_{\lambda\in(\lambda_1,\lambda_2)} |\Gamma_\mathrm{dB}(\lambda)|$ is the minimum allowed return loss in the band (λ_1, λ_2).

Salisbury screen

Probably the simplest absorber is the Salisbury screen,

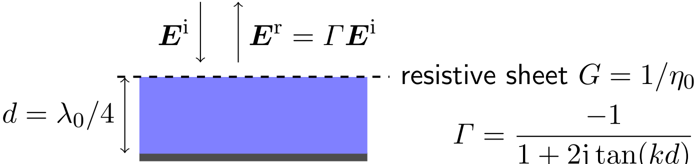

$$\mathit{\Gamma} = \frac{-1}{1 + 2\mathrm{j}\tan(kd)}$$

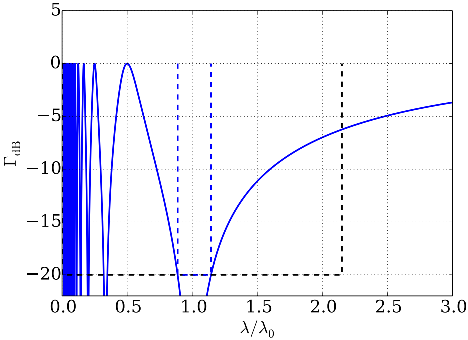

Reflection level $\mathit{\Gamma}_0 = 20\,\mathrm{dB}$ was chosen. Black dashed line is Rozanov's bound, blue dashed line achieved bandwidth $(\lambda_2 - \lambda_1) \approx 0.25\lambda_0$. This gives $\frac{(\lambda_2 - \lambda_1)\mathit{\Gamma}_0}{172d} = 12\%$.

Close to optimal absorber

A more wide band absorber was presented in [12], based on multilayer, capacitive patches.

- Total thickness $d = 14.5\,\text{mm}$, target level $\Gamma_0 = 20\,\text{dB}$.
- Lower frequency $f_\text{L} = 3.26\,\text{GHz} \Rightarrow \lambda_2 = 9.20\,\text{cm}$.
- Upper frequency $f_\text{H} = 34.65\,\text{GHz} \Rightarrow \lambda_1 = 8.65\,\text{mm}$.

Product of longest wavelength and reflection level $\lambda_2\Gamma_0/(172d) = 74\%$.

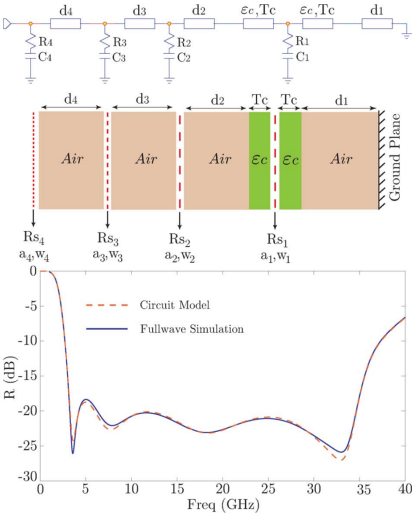

Outline

A similar bound for transmission blockage

Consider transmission through a periodic structure, designed to block electromagnetic waves at some frequency [10, 15].

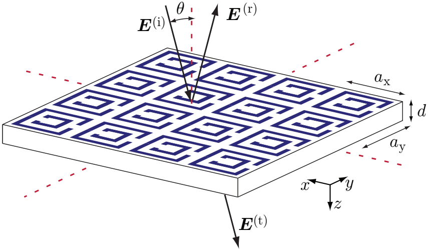

For a low pass structure ($T(0) = 1$), we can bound the transmission blockage much in the same way as the absorption of an absorber:

$$(\lambda_2 - \lambda_1) \ln \frac{1}{T_0} \leq \frac{\pi^2 \gamma(\theta)}{2A \cos\theta} - \left(\sqrt{n_\infty^2 - \sin^2\theta} - \cos\theta \right) d$$

Sum rule

With unconnected metal structures, we have asympotics

$$T(k) = \begin{cases} 1 - \frac{\mathrm{j}k\gamma(\theta)}{2A\cos\theta} + \mathrm{O}(k^2) & k \to 0 \\ \mathrm{e}^{-\mathrm{j}(n_\infty - 1)kd\cos\theta} + \mathrm{O}(1/k) & k \to \infty \end{cases}$$

where the angle-dependent polarizability is

$$\gamma(\theta) = \begin{cases} \gamma_{\mathrm{e}xx}\cos^2\theta + \gamma_{\mathrm{e}zz}\sin^2\theta + \gamma_{\mathrm{m}yy}, & \mathrm{TM} \\ \gamma_{\mathrm{e}yy} + \gamma_{\mathrm{m}xx}\cos^2\theta + \gamma_{\mathrm{m}zz}\sin^2\theta, & \mathrm{TE} \end{cases}$$

As with the absorber case, we need to eliminate possible zeros:

$$T'(k) = T(k)\frac{(k-k_1^*)\cdots(k-k_N^*)}{(k-k_1)\cdots(k-k_N)}$$

The sum rule for transmission blockage is then

$$\underbrace{\int_0^\infty \ln\frac{1}{|T(\lambda)|}\,\mathrm{d}\lambda}_{\geq(\lambda_2-\lambda_1)\ln\frac{1}{T_0}} \leq \frac{\pi^2\gamma(\theta)}{2A\cos\theta} - \left(\sqrt{n_\infty^2 - \sin^2\theta} - \cos\theta\right)d$$

Angle-dependent polarizability

The angle-dependent polarizability

$$\gamma(\theta) = \begin{cases} \gamma_{\mathrm{e}xx}\cos^2\theta + \gamma_{\mathrm{e}zz}\sin^2\theta + \gamma_{\mathrm{m}yy}, & \text{TM} \\ \gamma_{\mathrm{e}yy} + \gamma_{\mathrm{m}xx}\cos^2\theta + \gamma_{\mathrm{m}zz}\sin^2\theta, & \text{TE} \end{cases}$$

is a combination of in-plane polarizabilities (xy-components), and normal polarizabilities (z-components). The in-plane polarizabilities can typically be estimated by the polarizability of enclosing patches, due to the variational principle:

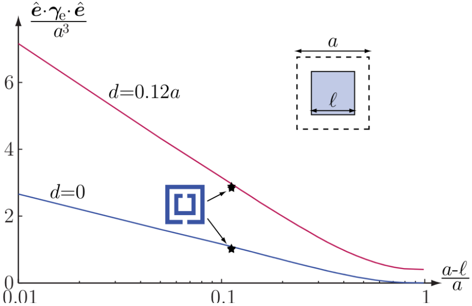

Experimental verification of transmission blockage

The sum rule has been experimentally verified. Split-ring patterns were designed, manufactured, and measured.

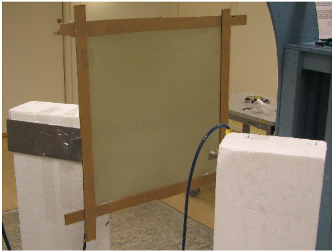

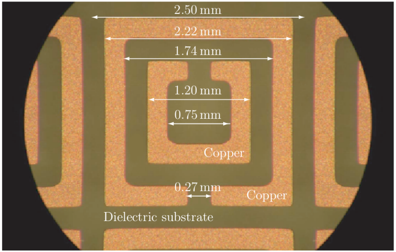

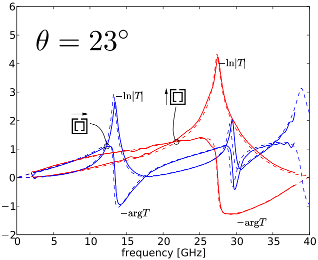

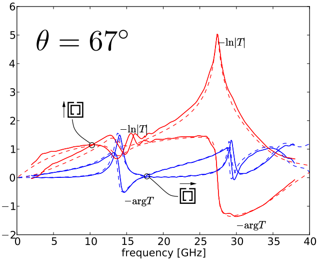

Results for different angles

Define the blockage by (the actual integration interval is bounded)

$$\frac{\cos\theta}{\pi^2}\int_0^\infty \ln\frac{1}{|T(\lambda)|}\,\mathrm{d}\lambda$$

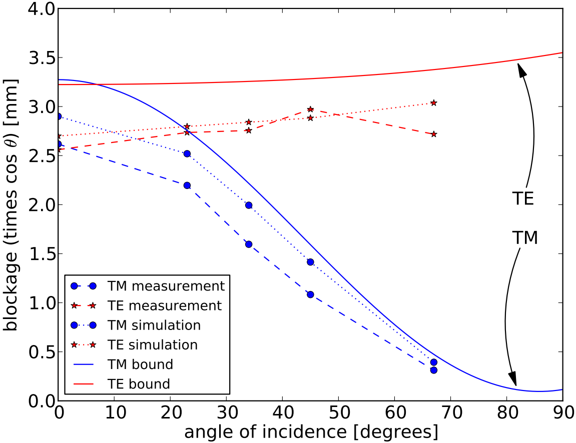

Note the significant decrease with angle for TM polarization.

Outline

High-impedance surfaces

A metal ground plane has reflection coefficient $\Gamma = -1$. In order to stop surface waves or reduce the thickness of planar antennas, it is desirable with $\Gamma = +1$.

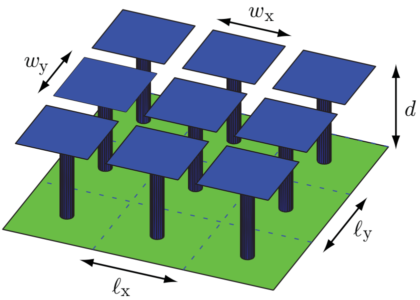

Loading the ground plane with a structure like patches on vias can do the trick, but with limited bandwidth [7]:

$$\boxed{\frac{\lambda_2 - \lambda_1}{d} \le \pi}$$

Low frequency asymptotic

For analysis, the ground plane can be removed by mirroring the geometry and adding an extra incident field from below. Note that the static applied field then is

$$\boldsymbol{E} = 2E_z^{\mathrm{i}}\hat{\boldsymbol{z}}$$

$$\boldsymbol{H} = 2\boldsymbol{H}_{\mathrm{xy}}^{\mathrm{i}}$$

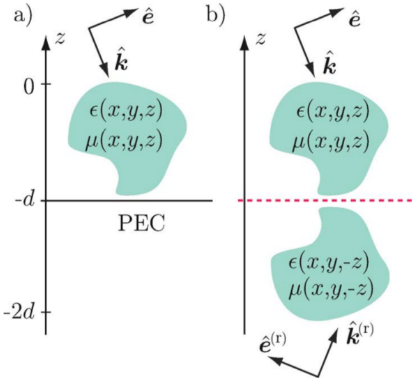

The low frequency asympotic for the reflection coefficient is

$$\varGamma(s) = -1 + \frac{2sd}{\mathrm{c}}\left(\cos\theta + \frac{\gamma(\theta)}{2A\cos\theta}\right) + \mathrm{O}(s^2), \quad s \to 0$$

where

$$\gamma(\theta) = \begin{cases} \gamma_{\mathrm{e}zz}\sin^2\theta + \gamma_{\mathrm{m}yy} & \mathrm{TM} \\ \gamma_{\mathrm{m}xx}\cos^2\theta & \mathrm{TE} \end{cases}$$

Transformation of the reflection coefficient

We want to characterize when $\Gamma \approx +1$, or when the normalized surface admittance

$$\frac{Y(s)}{Y_{\mathrm{t}}(\theta)} = \frac{1-\Gamma(s)}{1+\Gamma(s)} \approx 0, \quad Y_{\mathrm{t}} = \begin{cases} 1/\cos\theta & \mathrm{TM} \\ \cos\theta & \mathrm{TE} \end{cases}$$

We observe that $Y(s)$ is a positive real function, and apply the composition

$$P_{\Delta}(Y(s)) = \frac{2}{\pi}\arctan\left(\frac{\Delta}{Y(s)}\right)$$

The function $\mathrm{Re}\,P_{\Delta}$ is an indicator of when its argument is smaller than Δ.

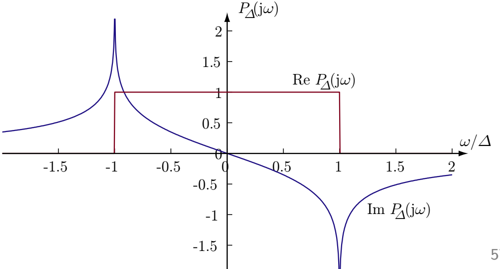

Sum rule for the composite function

Using the low frequency asymptotic of $\Gamma(s)$, and that $Y(s)$ grows at most linearly with s, we obtain

$$P_\Delta(Y(s)) = \begin{cases} \frac{2sd}{c\pi Y_t(\theta)}\left(\cos\theta + \frac{\gamma(\theta)}{2A\cos\theta}\right) + o(s) & s \to 0 \\ o(s) & s \to \infty \end{cases}$$

This gives the sum rule

$$\boxed{\int_0^\infty \mathrm{Re}\, P_\Delta(Y(\lambda))\,\mathrm{d}\lambda = \left(d\cos\theta + \frac{\gamma(\theta)}{2A\cos\theta}\right)\frac{2\pi\Delta}{Y_t(\theta)}}$$

For nonmagnetic, lossless structures and $\Delta = 1/2$, the right hand side can be estimated by πd, and we have the physical bound

$$\boxed{\frac{\lambda_2 - \lambda_1}{d} \leq \pi}$$

Example: quarter-wavelength slab

The simplest realization of a high-impedance surface is by simply shifting the reference plane one quarter wavelength.

The figures illustrate the behavior of $\mathrm{Re}\, P_\Delta(Y)$ as function of both frequency and wavelength.

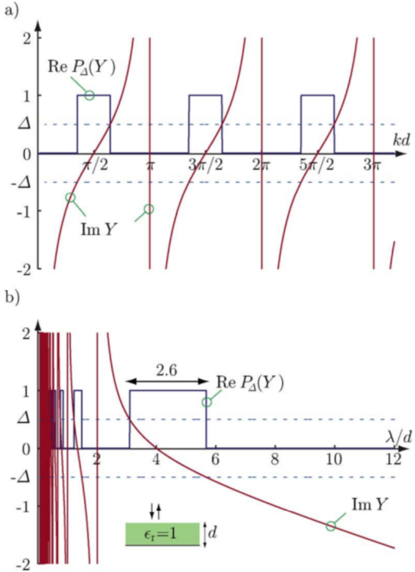

Example: mushroom surface

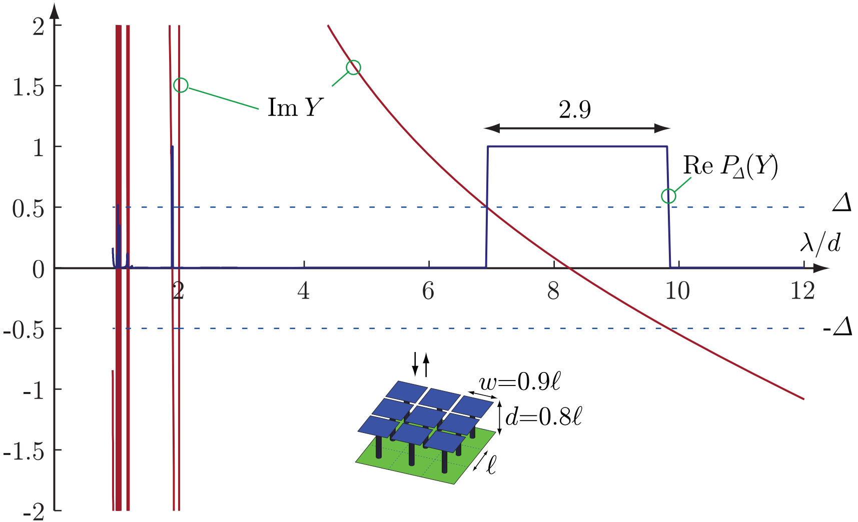

Example: dependence on angle of incidence

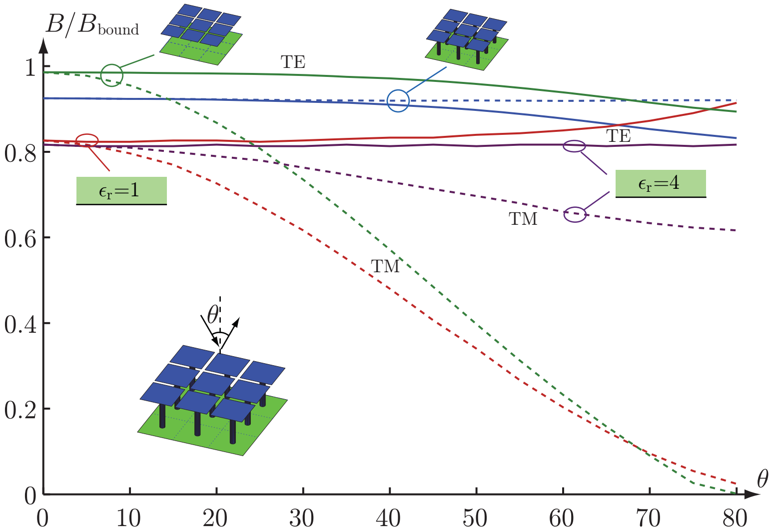

Outline

Typical frequency dependence for dielectrics:

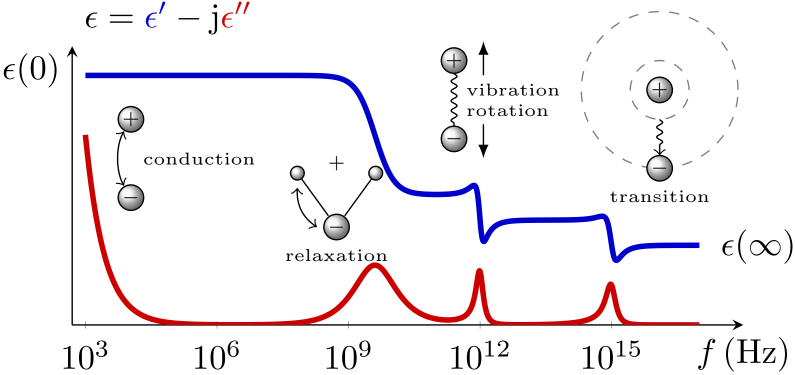

Metamaterials

Typical frequency dependence for dielectrics:

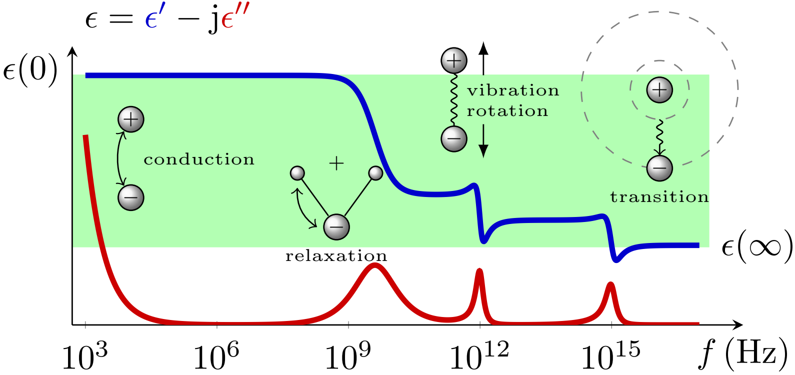

It is difficult to create materials with a response outside the region $[\epsilon(\infty), \epsilon(0)]$.

Physical bounds on metamaterials [6]

With no knowledge of ϵ_s (typically, a conductor), and target permittivity $\epsilon_\mathrm{m} < \epsilon_\infty$, we have

$$\max_{\omega\in\mathcal{B}} |\epsilon(\omega) - \epsilon_\mathrm{m}| \geq \frac{B}{1+B/2}(\epsilon_\infty - \epsilon_\mathrm{m}) \begin{cases} 1/2 & \text{lossy case} \\ 1 & \text{lossless case} \end{cases}$$

For an insulator (where ϵ_s is well defined), when $\epsilon_\mathrm{m} < \epsilon_\infty$

$$\max_{\omega\in\mathcal{B}} \frac{|\epsilon(\omega) - \epsilon_\mathrm{m}|}{|\epsilon(\omega) - \epsilon_\infty|} \geq \frac{B}{1+B/2}\frac{\epsilon_\mathrm{s} - \epsilon_\mathrm{m}}{\epsilon_\mathrm{s} - \epsilon_\infty} \begin{cases} 1/2 & \text{lossy case} \\ 1 & \text{lossless case} \end{cases}$$

When $\epsilon_\mathrm{m} > \epsilon_\mathrm{s}$:

$$\max_{\omega\in\mathcal{B}} \frac{|\epsilon(\omega) - \epsilon_\mathrm{m}|}{|\epsilon(\omega) - \epsilon_\infty|} \geq \frac{B}{1+B/2}\frac{\epsilon_\mathrm{m} - \epsilon_\mathrm{s}}{\epsilon_\mathrm{s} - \epsilon_\infty} \begin{cases} 1/2 & \text{lossy case} \\ 1 & \text{lossless case} \end{cases}$$

Outline

Exercises

The following exercises can with advantage be solved using matlab, python, or similar software. Some hints are available in the references of this presentation.

Exercise 1

Consider two absorber designs, a Salisbury screen and a Dällenbach absorber (a homogeneous lossy dielectric slab). How close do they come to Rozanov's bound? Illustrate the results with some graphs.

- Salisbury screen: $\mathit{\Gamma} = -1/(1 + 2\mathrm{j}\tan(kd))$ with $k = \omega/\mathrm{c} = 2\pi/\lambda$ being the wave number in free space, and d is the thickness of the absorber.
- Dällenbach absorber: $\mathit{\Gamma} = (1 - Y)/(1 + Y)$, where the relative surface admittance is $Y = n/(\mathrm{j}\tan(nkd))$ with $n = \sqrt{\epsilon_\mathrm{r}}$ being the refractive index. The relative permittivity $\epsilon_\mathrm{r}(\omega)$ needs to be lossy and depend on frequency, one choice can be $\epsilon_\mathrm{r} = 1 + 1.76/(\mathrm{j}kd)$, but feel free to try other.

Exercise 2

Consider a dielectric slab with thickness 0.3 mm, with either constant relative permittivity 4.35, or frequency-dependent $\epsilon_\mathrm{r}(\omega) = 1 + 3.35/(1 + \mathrm{j}\omega/\omega_\mathrm{c})$ with $\omega_\mathrm{c} = 2\pi\mathrm{c}/(1\,\mu\mathrm{m})$, where c is the speed of light in vacuum. Compute the angle-dependent polarizability per unit area and thickness, $\gamma(\theta)/(Ad)$, and high-frequency refractive index n_∞. Compare the integrated transmission blockage with the bound in the two cases.

Outline

References I

[1] A. Bernland, M. Gustafsson, and S. Nordebo.
Physical limitations on the scattering of electromagnetic vector spherical waves.
J. Phys. A: Math. Theor., 44(14):145401, 2011.

[2] H. W. Bode.
Network analysis and feedback amplifier design, 1945.
Van Nostrand, 1945.

[3] R. M. Fano.
Theoretical limitations on the broadband matching of arbitrary impedances.
Journal of the Franklin Institute, 249(1,2):57–83 and 139–154, 1950.

[4] M. Gustafsson.
Sum rule for the transmission cross section of apertures in thin opaque screens.
Opt. Lett., 34(13):2003–2005, 2009.

[5] M. Gustafsson.
Sum rules for lossless antennas.
IET Microwaves, Antennas & Propagation, 4(4):501–511, 2010.

[6] M. Gustafsson and D. Sjöberg.
Sum rules and physical bounds on passive metamaterials.
New Journal of Physics, 12:043046, 2010.

[7] M. Gustafsson and D. Sjöberg.
Physical bounds and sum rules for high-impedance surfaces.
IEEE Trans. Antennas Propagat., 59(6):2196–2204, 2011.

[8] M. Gustafsson, C. Sohl, and G. Kristensson.
Physical limitations on antennas of arbitrary shape.
Proc. R. Soc. A, 463:2589–2607, 2007.

[9] M. Gustafsson, C. Sohl, and G. Kristensson.
Illustrations of new physical bounds on linearly polarized antennas.
IEEE Trans. Antennas Propagat., 57(5):1319–1327, May 2009.

[10] M. Gustafsson, C. Sohl, C. Larsson, and D. Sjöberg.
Physical bounds on the all-spectrum transmission through periodic arrays.
EPL Europhysics Letters, 87(3):34002 (6pp), 2009.

References IV

[11] M. Gustafsson, I. Vakili, S. E. B. Keskin, D. Sjöberg, and C. Larsson.
Optical theorem and forward scattering sum rule for periodic structures.
IEEE Trans. Antennas Propagat., 60(8):3818–3826, 2012.

[12] A. Kazemzadeh.
Nonmagnetic ultra wideband absorber with optimal thickness.
IEEE Trans. Antennas Propagat., 59(1):135–140, 2011.

[13] K. N. Rozanov.
Ultimate thickness to bandwidth ratio of radar absorbers.
IEEE Trans. Antennas Propagat., 48(8):1230–1234, Aug. 2000.

References V

[14] D. Sjöberg.
Variational principles for the static electric and magnetic polarizabilities of anisotropic media with perfect electric conductor inclusions.
J. Phys. A: Math. Theor., 42:335403, 2009.

[15] D. Sjöberg, M. Gustafsson, and C. Larsson.
Physical bounds on the all-spectrum transmission through periodic arrays: Oblique incidence.
EPL Europhysics Letters, 92:34009 (6pp), 2010.

[16] C. Sohl, M. Gustafsson, and G. Kristensson.
Physical limitations on broadband scattering by heterogeneous obstacles.
J. Phys. A: Math. Theor., 40:11165–11182, 2007.

References VI

[17] C. Sohl, C. Larsson, M. Gustafsson, and G. Kristensson.
A scattering and absorption identity for metamaterials: experimental results and comparison with theory.
J. Appl. Phys., 103(5):054906, 2008.

[18] I. Vakili, M. Gustafsson, D. Sjöberg, R. Seviour, M. Nilsson, and S. Nordebo.
Sum rules for parallel-plate waveguides: Experimental results and theory.
IEEE Transactions on Microwave Theory and Techniques, 62(11):2574–2582, 2014.